J Solid State Electrochem (2007) 11:1705–1712
DOI 10.1007/s10008-007-0347-8

ORIGINAL PAPER

Electroless Ni–P coated on graphite as catalyst for the electro-oxidation of dextrose in alkali solution

G. Veera Babu · M. Palaniappa · M. Jayalakshmi · K. Balasubramanian

Received: 26 February 2007 / Revised: 30 March 2007 / Accepted: 27 April 2007 / Published online: 15 May 2007

Abstract Graphite particles were coated with Ni–P by electroless deposition using a conventional bath consisting of a nickel salt and hypophosphite. After 15 min of electroless deposition, the graphite particles were covered with 10 wt% nickel and 0.7–1.0 wt% phosphorus as analysed by wet chemical method. Surface morphology was studied by scanning electron microscopy (SEM). Electrochemical characterisation for the catalytic activity was done by cyclic voltammetry. Pure Ni powder and electroless Ni–P coated on graphite were used as catalysts for the electro-oxidation of dextrose (1.8×10^{-3} to 4.5×10^{-3} M) in 0.1 M KOH solution. Comparative studies revealed that electroless Ni–P coated on graphite particles acted as a better catalyst than pure Ni powder for catalytic reaction.

Keywords Electroless Ni–P · Graphite particles · Electro-catalysis · Dextrose · Alkali solution

Introduction

Electroless nickel plating (EN) is an autocatalytic chemical reduction process in which the reducing agent is oxidised and Ni^{2+} ions are deposited (reduced) on the substrate surface. Once the first layer of Ni is deposited, it acts as a catalyst for the process. The vast majority of EN coatings are deposited by catalytic reduction of nickel ions with sodium hypophosphite (NaH_2PO_2). From published tables of standard electrode potentials, the hypophosphite ion ($H_2PO_2^-$) has a redox potential of −0.5 V and so, theoretically, is strongly reducing to nickel ions (−0.25 V) under standard conditions [1, 2]. However, at normal bath conditions, there is no reduction of nickel ions by hypophosphite despite the significant thermodynamic driving force derivable from the standard electrode potentials [3]. This is due to the fact that hypophosphite ions possess a remarkable inertia towards electrochemical oxidation in aqueous solutions [4]. Once the initial nickel layer has deposited on the catalytic substrate, it acts as a catalyst for the process, and the deposition continues to propagate unaided. This is referred to as autocatalysis of the deposition reaction, but it has been postulated that it occurs in microcells of alternating anodic/cathodic polarity on the surface of the substrate. This unique property of EN plating makes it possible to coat internal surfaces of pipes, valves, nuts and bolts and other complex geometries that are very difficult or impossible to be coated by conventional electroplating techniques.

Several theories were proposed for the mechanism of the electroless nickel process with hypophosphite as a reducing agent. Brenner and Riddell [5] gave the following equation for the electroless deposition of nickel from a solution containing a nickel salt and hypophosphite; the credit of introducing EN to the world goes to these authors, as they were the ones who completed the first laboratory experiment in 1944:

$$Ni^{2+} + H_2PO_2^- + H_20 \rightarrow Ni + H_2PO_3^- + 2H^+. \quad (1)$$

G. V. Babu · M. Palaniappa (✉) · M. Jayalakshmi · K. Balasubramanian
Non-Ferrous Materials Technology Development Centre,
Kanchanbagh Post,
Hyderabad 500 058, India
e-mail: mpalaniappa@nftdc.res.in

Hydrogen is simultaneously evolved. According to Brenner, this occurs by the side reaction,

$$H_2PO_2^- + H_20 \rightarrow H_2PO_3^- + H_2. \quad (2)$$

The deposited nickel contains phosphorus. Reactions suggested for the co-deposition of phosphorus are,

$$3H_2PO_2^- \rightarrow H_2PO_3^- + 2P + H_2O + 2OH^- \quad (3)$$

or

$$H + H_2PO_2^- \rightarrow P + OH^- + H_2O \quad (4)$$

Several theories are put forward to explain the mechanism of the process. Neglecting the deposition of P for the sake of simplicity, the reactions can be written as,

$$\text{Cathodic} : Ni^{2+} + 2\,e \rightarrow Ni^0 \quad (5)$$

$$2H^+ + 2\,e \rightarrow H_2 \quad (6)$$

$$\text{Anodic} : H_2PO_2^- + H_20 \rightarrow H_2PO_3^- + 2H^+ + 2\,e. \quad (7)$$

An in situ UV-Vis spectroscopic study confirmed the formation of the intermediate PHO_2^- during the electro-catalytic oxidation mechanism [6].

The technological importance of EN coating on graphite particles is envisaged by the application of this composite material as anode in Li-ion batteries [7, 8]. When nanosized nickel (10 wt%) is deposited on a graphite surface by reduction with sodium hypophosphite, this coating or encapsulation covers the surface of graphite particles and blocks effectively the edge surfaces from the exposure of graphite surface to the electrolyte solution. Solvent molecules cannot pass through this coating, and the co-intercalation of the solvated lithium ions via the edge sites of graphite, the subsequent reduction of propylene carbonate (PC), the exfoliation of the graphene layers and gas evolution are greatly minimised. As a result, the charge–discharge performance of the anode is improved, and the explosions from the large production of gases are avoided [7]. In addition, this kind of coating is metallic Ni, a good conductor, and it leads to an increase in exchange current densities and diffusion coefficients of the lithium ions and a decrease of the charge-transfer resistance and the surface film resistance in comparison with bare graphite. The composite exhibits less capacity loss over a 10-day storage period. In addition, the conductivity of the composites is increased in comparison with bare graphite, and good electrochemical performance at large current or high-rate capability is observed [8, 9].

To our knowledge, similar reports on the electro-catalytic activity of EN/graphite composite are not available, although the electro-catalytical behavior of Ni–P coatings towards hydrogen evolution reaction (HER) is reported by many authors [10–13]. The main aim of this investigation is to study the electro-catalytic behavior of EN/graphite composite prepared by electroless deposition; this is actually a Ni–P alloy deposited on graphite particles. Graphite is known to enhance the conductivity and surface area, and the strategy to know its actual role is to compare the electro-catalytic performance of EN/graphite composite with that of pure Ni. Conventionally, for materials that do not have catalytic surface, before actual plating, a sensitisation step ($SnCl_2$) followed by activation ($PdCl_2$) was done. Ceramic substrates such as SiC [14], Al_2O_3 [15] and carbon nano-tubes [16] and graphite [17] are some of the reported examples. In the present work, the activation of graphite particles is done by a different technique without the use of sensitisation and activation, which was adopted by us in our earlier work and gave good results [18]. Dextrose is chosen as the model compound to study the electro-catalytic behavior in 0.1 M KOH solution by cyclic voltammetry. Surface morphology of the EN/graphite is done by scanning electron microscopy (SEM). Brunauer–Emmett–Teller (BET) surface areas of EN/graphite, pure Nickel and graphite are measured. Ni content in the EN/graphite was determined from wet chemical method, while P content was measured by inductively coupled plasma–atomic emission spectrometry (ICP-AES) analysis.

Experimental

Electroless deposition

Graphite particles were subjected to activation before electroless plating. The activation process was carried out by heating the graphite particles in a muffle furnace at 380 °C for 1 h in air atmosphere [18]. This exercise was done to drive off the adsorbed gases on the surface of graphite particle to ensure a clean active surface, which enhances the wettability of the powders in the aqueous solution. After pretreatment (activation), graphite powders were introduced into the electroless nickel-plating bath. Electroless nickel was plated using a sodium hypophosphite bath, and the composition of the bath is given in Table 1. Nickel sulphate

Table 1 Chemical composition of Electroless Ni–P plating bath

Chemical	Formula	Quantity (g/l)
Nickel sulphate	$NiSO_4{\cdot}6H_2O$	10
Tri-sodium citrate	$Na_3C_6H_5O_7{\cdot}H_2O$	15
Ammonium sulphate	$(NH_4)_2SO_4$	15
Sodium hypophosphite	$NaH_2PO_2.H_2O$	16

was the source for metal ions, sodium hypophosphite was the reducing agent, sodium citrate was used as a complexing agent and ammonium sulphate acts as a buffering agent to control pH of the bath during plating process. The chemicals used in this experiment were all analytical reagent grade products. The electroless plating was performed on a hot plate with a magnetic stirrer by maintaining the temperature of the bath at 85±2 °C. Effect of plating time, weight of graphite powder and composition of the plating bath solution were studied. After electroless plating, the suspension was filtered, washed thoroughly with distilled water several times and dried in an oven at 90 °C for 2 h. The pH of the plating bath was in the range of 5.5–6.0. The composition of the deposited nickel on the graphite powders was analysed by wet chemical method.

Wet chemical method was carried out as follows: About 0.1 g of the composite was dissolved in 1:1 HNO_3, and the undissolved graphite was filtered out. The filtrate containing Ni and P was made up to 100 ml volume in a standard volumetric flask. For Ni analysis, 20 ml of this solution was taken in a conical flask, and the pH was adjusted to 6.5 by adding hexamine. This solution was complexed with ethylenediaminetetraacetic acid (EDTA). With PAR as indicator, excess EDTA was back titrated with lead nitrate for determining the amount of Ni content in the EN/graphite.

Instrumentation

All electrochemical experiments were conducted with a PGSTAT 302 Autolab system (Ecochemie, Utrecht, The Netherlands). It was connected to a PC running with Eco-Chemie GPES software. GPES software was used for all electrochemical data analysis. The reference electrode was Ag/AgCl (3 M KCl), and the counter electrode was a platinum wire supplied along with the instrument. Paraffin impregnated graphite electrodes (PIGE) were used as working electrodes with the surface immobilised with the active electrode materials. A few micrograms of Ni and Ni–P coated graphite particles were placed on a clean glass plate, and the surface of PIGE electrode was pressed over the powders, which would mechanically transfer the microparticles to the tip of the electrode [19]. Cyclic voltammograms (CVs) were traced on the modified electrode in the potential range of 0.1 to 0.9 V in a background electrolyte of KOH solution at a scan rate of 50 mV/s for ten cycles. All measurements were performed at ambient temperatures. The BET surface area was measured with a Quantachrome Autosorb-1 Model using the single point method. SEM images were obtained with a Hitachi (Japan) model. ICP-AES analysis was1,540 done in IRIS Intrepid II XDL model from Thermo Electronic, USA.

Results and discussion

Electroless deposition

Electroless Ni deposition proceeds without any external electrodes, but there is electric charge transfer involved. In place of an anode, there is Ni provided by its salt in solution. In place of a cathode, there is the graphite substrate while the electrons are provided by the reducing agent (hypophosphite) in the solution. Both the anode and cathode reactions take place at the graphite/solution interface. The deposition of Ni on graphite to form an EN/graphite composite is governed by a two-step adsorption mechanism. In the first step, the dispersed particles (Ni^{2+}) in the bath are transported to the surface of the electrode (graphite) by mechanical action and are physically adsorbed due to the fluidal contact. In the second step, these physically adsorbed particles dehydrate because of the strong electric field of Helmholtz layer of the substrate, and a strong irreversible chemical adsorption of particles on the electrode takes place. The physical adsorption is Langmuir adsorption, while the chemical adsorption is Temkin adsorption. The amount of physically adsorbed particle on the electrode is much larger than the chemically adsorbed ones. Xinguo and Naichao [20] have shown that only a fraction of the physically adsorbed particles get converted into chemically adsorbed particles.

Ni^{2+} ions adsorbed on the graphite surface were reduced by the hypophosphite anion, forming the first layer of metallic Ni on the graphite surface. Once the deposition starts, this layer of Ni acts as a catalyst for the deposition to continue. The most important point is that the catalytic or activated surface site is the only place where this simplified reaction occurs; this means that the entire graphite surface would not be activated in unison. The deposition of NiP starts at specific activation sites on the surface and continues at these points only. As deposition progresses, islands are formed around these nucleation sites. As the deposits grow linear in time, if sufficient time is given, the islands grow in size until they merge and a continuous film results (if sufficient time window for the experiment is provided). From our SEM images, our composite did not form a continuous film but discrete islands. This result is consistent with an earlier report where the microencapsulation of NiP on graphite surface depressions as clusters [7].

The adsorbed Ni^{2+} ions in the presence of the activated catalytic surface is reduced by the adsorbed hypophosphite ions, and the plating proceeds so long as there is sufficient availability of metal ions and reducing agent. Nickel reduction on the surface is confirmed by the evolution of hydrogen from the substrate surface. In this case, initially, very vigorous reaction was observed during the electroless deposition. The plating rate increases with increase in time

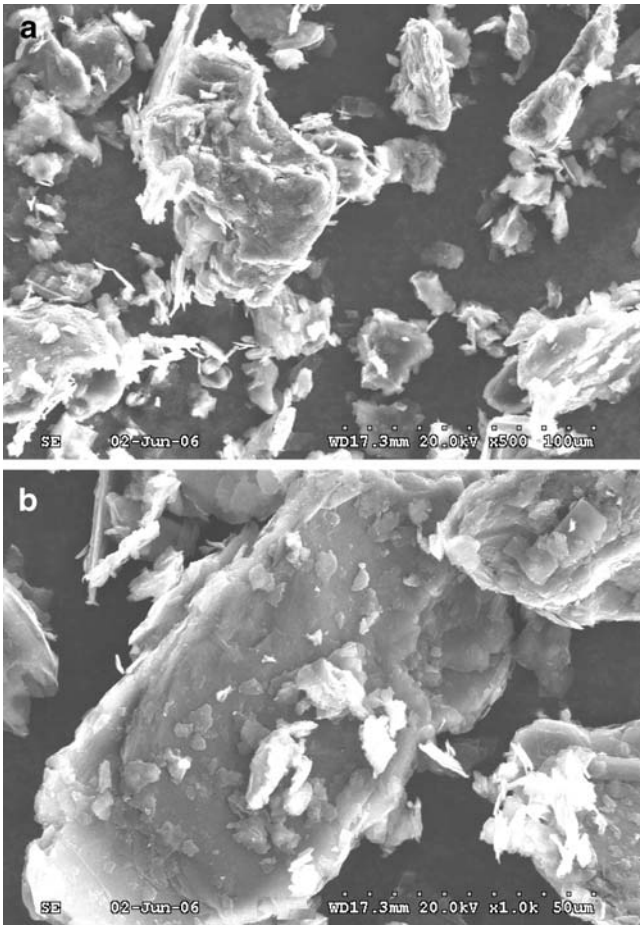

Fig. 1 SEM micrographs of uncoated graphite powders. **a** Magnification × 500; **b** magnification × 1,000

but approaches a limiting value after a time window of 15 min. This can be attributed to depletion of metal ion and reducing agent in the bath as a function of time. However, the nickel content on the powder can be further increased by removing the powder after 15–30 min plating, washing with distilled water and continuing plating in a fresh solution or by replenishing the existing bath with sufficient metal ions. Nickel content in the EN/graphite composite was 10 wt%, and the amount of phosphorus was in the range of 0.7–1.0 wt%. From our earlier work on varying on Ni and P contents, this P composition gives rise to amorphous deposit [21], which may hold well in this work also.

BET surface area

The BET surface area of pure Ni powder used in this study was 10.4 $m^2\ g^{-1}$ while that of activated graphite powder was 14.8 $m^2\ g^{-1}$. For electroless NiP coated on graphite, the surface area was 12.2 $m^2\ g^{-1}$. The surface area of NiP–graphite composite is higher than that of pure Ni but lower than that of activated graphite. The decrease in surface area of the NiP–graphite is understandable, as the nanometer-sized NiP particles deposited on the active surface sites of graphite particles tend to decrease the exposed surface of the graphite.

SEM images

Figure 1a and b shows the particles of graphite before coating in two different magnifications. The shapes of the graphite particles were not uniform, and their size distribution was in the range of 50–150 μm. After electroless deposition, the graphite particles had tiny spheres of nickel grains deposited over them as shown in Fig. 2a and b, thus forming the EN/graphite composite. The metal being deposited as islands can be visualised as cauliflower structure on the surface of graphite particles, which was more clearly visible at higher magnification (Fig. 3). Given that the particle size of graphite was in the range of 50–150 μm, the grain size of nickel was found to be in the range of 15–50 nm.

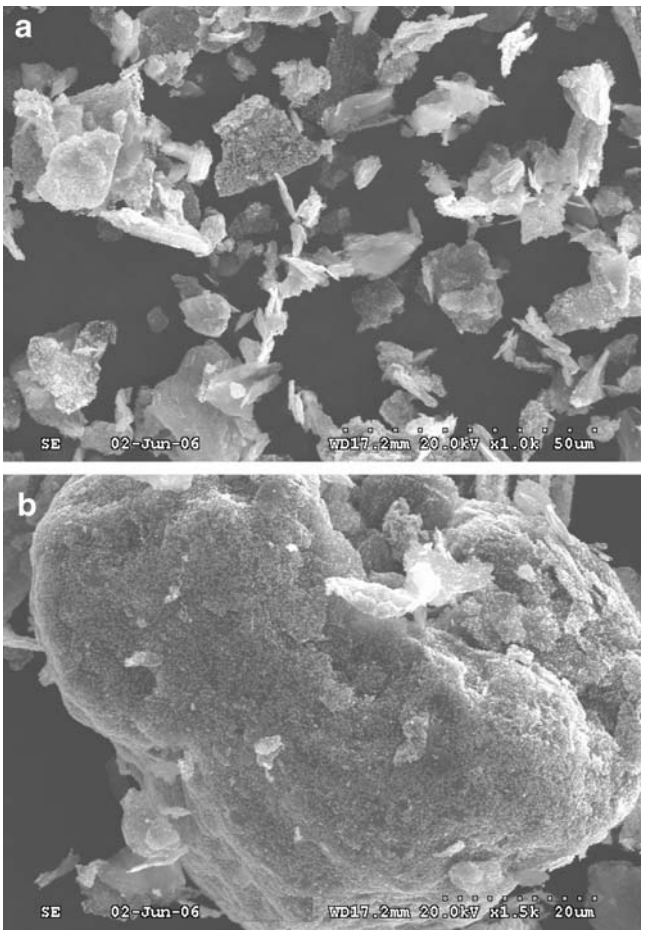

Fig. 2 SEM micrographs of coated graphite powders. **a** Magnification × 1,000; **b** magnification × 1,500

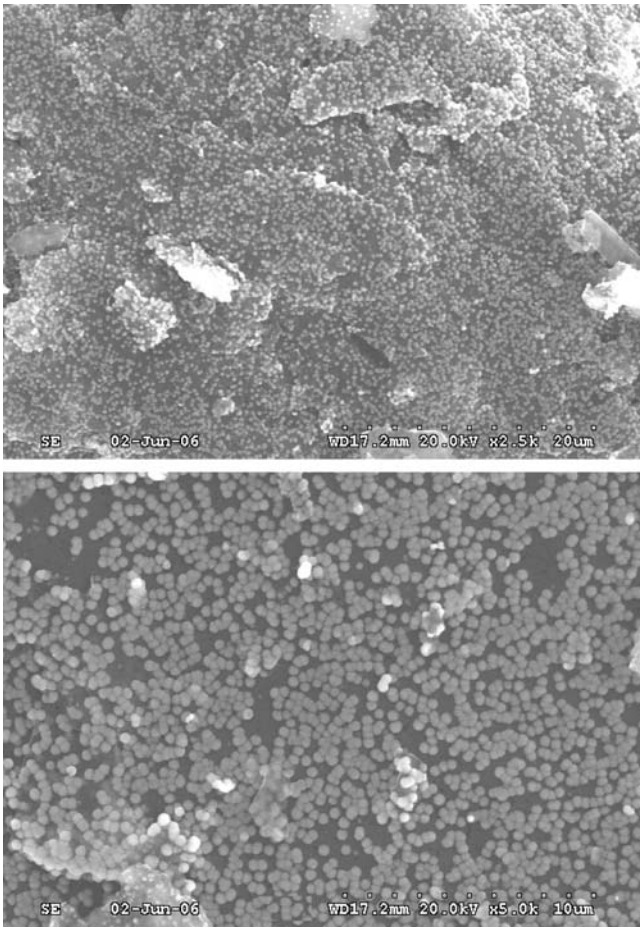

Fig. 3 SEM micrographs of coated graphite powders at higher magnification showing the cauliflower structure of Ni–P deposit

Electrochemical characterisation

The electrochemistry of Ni in alkali solution is a well-studied subject due to its application as cathode in Ni–Fe and Ni–Cd secondary batteries. Exhaustive literature is available on this topic. The purpose of presenting these CVs in the present study is to understand the differentiation in the electrochemical behavior of pure Ni powder and electroless Ni–P coated on graphite particles. Figure 4 shows the CVs recorded for Ni/PIGE in 0.1 M KOH solution. The CVs get stabilised after ten cycles. The increase in peak currents after ten cycles may be ignored, as the increments were insignificant. For the stabilised response (tenth scan), the anodic peak appeared at 0.542 V, and the corresponding cathodic peak appeared at 0.27 V. The redox reaction responsible for the appearance of these peaks is

$$Ni(OH)_2 + OH^- \rightarrow NiOOH + H_2O + e^-$$

Shift of anodic peak potentials towards more positive potentials on continuous cycling was expected for the ageing process, i.e. the conversion of α- to β-phase. The anodic peak appeared at 0.494 V in the second scan, and the anodic charge under peak was 1.258×10^{-3} C, whereas the same peak appeared at 0.542 in the tenth scan with an incremental increase in charge of 3.341×10^{-3} C. This kind of electrochemical behavior is well known for Ni electrodes; as the α-phase is thermodynamically unstable, the conversion to the β-phase or a mixed phase is an energetically favourable process. Ironically, ΔEp also increases with cycling, an indication that the reversibility of the redox transformations decreased. It is a paradoxical situation but not unusual if one considers the complexity of the situation. The $Ni(OH)_2 \leftrightarrow NiOOH$ conversion itself is accompanied by influx of hydroxyl ions and outflux of water, protons, carbonate and nitrate ions in combination with ageing, which proceeds by two separate but complimentary processes, namely chemical ageing in KOH solution and electrochemical ageing between oxidised and reduced states [22, 23].

Figure 5 shows the CVs recorded for electroless Ni–P/graphite electrode for continuous ten cycles. The anodic and cathodic peaks were well defined, and the sharper peaks indicate charge transfer controlled mechanism. Unlike pure Ni, the anodic peak potentials appeared with a consistency, although the charges under the peak increased with cycling. The anodic peak appeared at 0.454 V in the second scan with a charge value of 4.907×10^{-4} C, while it appeared at 0.456 V in the tenth scan with an increased charge value of 8.483×10^{-4} C. These values indicate that the complexity in the pure Ni case does not exist here. Definitely, there was no indication of ageing, and increased reversibility indicates a lack of pronounced electrochemical ageing between oxidised and reduced

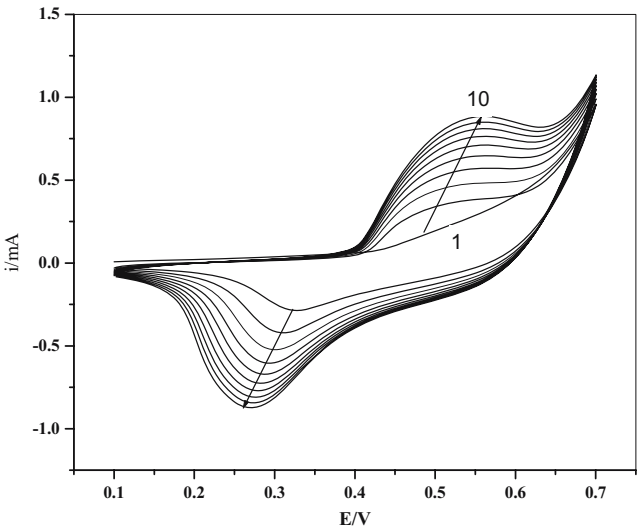

Fig. 4 Cyclic voltammograms (continuous cycling for ten scans) of Ni powder immobilized on PIGE electrode in 0.1 M KOH solution at 50 mV s^{-1}

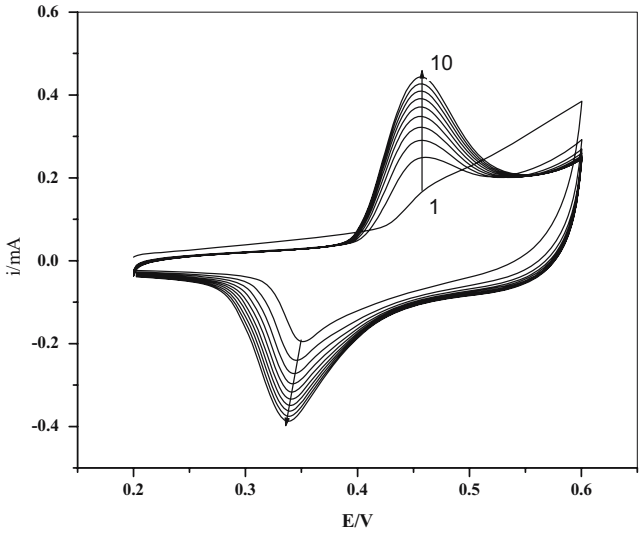

Fig. 5 Cyclic voltammograms (continuous cycling for ten scans) of Ni–P coated with graphite immobilized on PIGE electrode in 0.1 M KOH solution at 50 mV s^{-1}

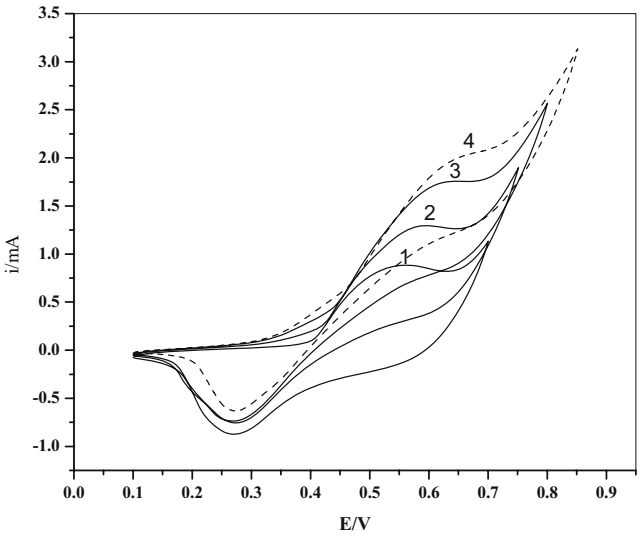

Fig. 6 Electro-catalytic behavior of pure Ni electrode in 1 M KOH and 1 M KOH+dextrose solutions; scan rate=50 mV s^{-1}; *curve 1* KOH; *curve 2* KOH+8.9×10^{-4} M dextrose; *curve 3* KOH+1.8×10^{-3} M dextrose; *curve 4* KOH+2.7×10^{-3} M dextrose

states. As stated in the introduction, this kind of Ni–P coating on graphite increases the conductance, exchange current densities and diffusion coefficients of hydroxyl ions and decreases the charge-transfer resistance and the surface film resistance as compared to bare graphite/pure Ni. Overall, the electrochemical performance of Ni was increased, although the cumulative charge reached at the stabilised tenth scan was not so different for both cases.

In this context, it is necessary to understand the fact that the α-phase of $Ni(OH)_2$ is not formed during the cyclic polarisation of NiP electrode. The extent of P content in the Ni–P seem to decide the possibility of α-phase of $Ni(OH)_2$ formation during cyclic voltammetric studies in alkali solutions. An elaborate study by A. M. Fundo and L. M. Abrantes showed that the cyclic voltammetric response of NiP with low P content (4.0 wt%) was similar to that of pure solid Ni (the above results were of powdered Ni), i.e. the adsorption of OH^- and conversion of Ni to α-$Ni(OH)_2$ did not occur for NiP with low P contents [13]. Another earlier report on NiP electrodes also claim that the most plausible reaction is β-$Ni(OH)_2$ to β-NiOOH [24]. In the present work, P content was in the range of 0.7–1.0 wt%, which seems to be an indirect proof that α-$Ni(OH)_2$ did not form and take part in the electro-catalytic reaction.

Figure 6 shows the CVs obtained for the catalytic response of pure Ni in the presence of dextrose in 0.1 M KOH solution, and Table 2 presents the peak potentials, peak currents and electro-catalytic efficiency (ECE) of the anodic peak. The ECE is defined as the ratio of the anodic catalytic current to the anodic peak current relative to the blank [25, 26]. From these data, the following observations were made: (1) the anodic peaks representing the oxidation of $Ni^{2+}\rightarrow Ni^{3+}$ shifts to more positive potentials with increase in concentration of dextrose added to the KOH solution; (2) likewise, the anodic peak currents increased steadily and reached a limiting value at the concentration of 3.6×10^{-3} M dextrose; (3) ECE increased in par with the peak current and reached a limiting proportion at the same concentration; (4) the cathodic peak remains unaffected except at higher concentrations of dextrose where it shifted to more positive potentials; (5) on the other hand, the reduction currents decreased prominently with every incremental addition of dextrose to the KOH solution.

These observations led us to believe that the catalytic oxidation of dextrose coincides with the oxidation of Ni$(OH)_2$ to NiOOH. In other words, dextrose is oxidised on the nickel electrode through the reaction with NiOOH to

Table 2 Anodic and cathodic peak (potential and current) and ECE (anodic) values for pure Ni powders

Electrolyte	Ni (anodic)			Ni (cathodic)	
	E_p (V)	I_p (mA)	ECE (×100)	E_p (V)	I_p (mA)
KOH	0.521	0.87	–	0.267	0.87
KOH + 0.89×10^{-3} M dex.	0.565	1.25	1.43	0.275	0.75
KOH + 1.8×10^{-3} M dex.	0.600	1.77	2.03	0.270	0.63
KOH + 2.7×10^{-3} M dex.	0.617	1.90	2.18	0.272	0.55
KOH + 3.6×10^{-3} M dex.	0.639	2.00	2.29	0.295	0.36
KOH + 4.5×10^{-3} M dex.	0.650	2.00	2.29	0.309	0.28

form $Ni(OH)_2$ [27, 28]. This explains the shift in anodic peak potentials towards positive direction as well as the increase in catalytic current with each incremental addition of dextrose to KOH solution. If this is the case, one expects that the cathodic peak should be affected because the NiOOH species required for the reduction at the cathodic peak was consumed during the catalytic process. This was noted to be true. Our results confirm the mechanism proposed by Fleischmann et al. [29, 30]. He suggested that NiOOH acts as an electro-catalyst. His ideas were mainly based on the experimental observation that alcohols and other organic compounds are oxidised at a potential, which coincided exactly with that where NiOOH was produced and on the disappearance of the NiOOH reduction peak in the cathodic sweep.

Figure 7 shows the CVs obtained for the catalytic response of EN/graphite in the presence of dextrose in 0.1 M KOH solution, and Table 3 presents the peak potentials, peak currents and ECE of the anodic peak for Ni–P. The general behavior remained the same except that the anodic peaks appeared at less positive potentials than for pure Ni. Furthermore, the anodic peak currents did not attain a limiting value but kept on increasing with the increase in dextrose concentrations in KOH solution. ECE reached a maximum of 6.11 at the highest dextrose addition, whereas it was only 2.29 for pure Ni. The cathodic peak potentials remained unaffected, but the peak currents decreased drastically in such a way that no cathodic peak appeared at the highest dextrose addition. EN/graphite behaves as a better electro-catalyst than pure Ni for the electro-oxidation of dextrose, which could be best seen from the CVs shown in Fig. 8. The CVs were that of pure Ni and EN\graphite at the highest dextrose concentration 4.5×10^{-3} M, which exemplifies the fact that EN\graphite is indeed a better electro-catalyst. The absence of oxidation peak in the case of pure Ni and both redox peaks in the case of EN\graphite suggests a surface coverage by dextrose molecules at the double layer especially at the solid side of interface, so that the formation of a redox peak, which requires the diffusion of electroactive species such as hydroxyl ion or protons, remains hindered. The fact that the catalytic current was higher for EN\graphite as against pure Ni is an indication of catalytic oxidation occurring at a rate faster than the rate of anodic peak formation.

Table 3 Anodic and cathodic peak (potential and current) and ECE (anodic) values for Ni–P coated graphite powders

Electrolyte	Ni (anodic)			Ni (cathodic)	
	E_p (V)	I_p (mA)	ECE (×100)	E_p (V)	I_p (mA)
KOH	0.454	0.45	–	0.338	0.37
KOH + 0.89×10^{-3} M dex.	0.500	1.10	2.44	0.329	0.32
KOH + 1.8×10^{-3} M dex.	0.546	1.56	3.47	0.325	0.25
KOH + 2.7×10^{-3} M dex.	0.594	2.05	4.55	0.324	0.19
KOH + 3.6×10^{-3} M dex.	0.632	2.50	5.56	0.295	0.36
KOH + 4.5×10^{-3} M dex.	0.675	2.75	6.11	–	–

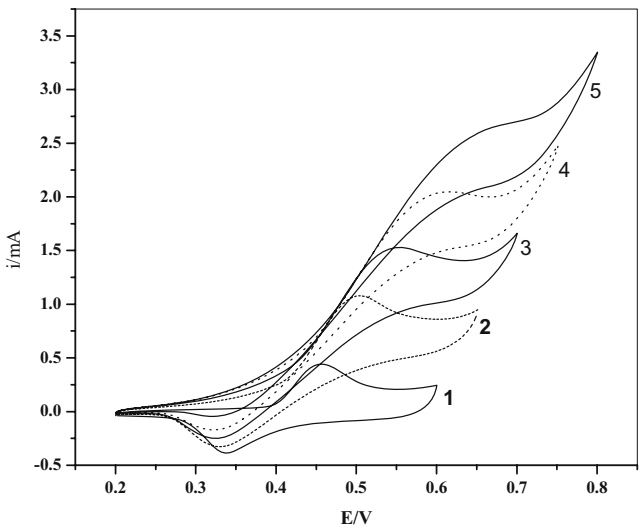

Fig. 7 Electro-catalytic behavior of Ni–P/PIGE electrode in 1 M KOH and 1 M KOH + dextrose solutions; scan rate=50 mV s^{-1}; *curve 1* KOH; *curve 2* KOH + 8.9×10^{-4} M dextrose; *curve 3* KOH + 1.8×10^{-3} M dextrose; *curve 4* KOH + 2.7×10^{-3} M dextrose; *curve 5* KOH + 3.6×10^{-3} M dextrose

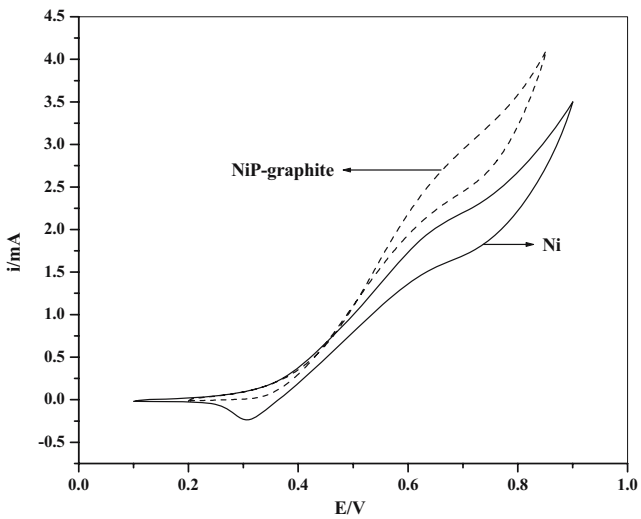

Fig. 8 Comparison of electro-catalytic behavior of pure Ni and NiP/graphite in 0.1 M KOH + 4.5×10^{-3} M dextrose solution at 50 mV s^{-1}

Conclusions

Ni–P has been deposited on graphite particles, which were activated by heating in air at 380 °C for 1 h. A 10 wt% nickel was deposited on graphite powders after 15 min of deposition time. Size of the Ni–P crystals was found to be in the range of 15–50 nm. Electro-catalytic behaviour of pure Ni and Ni–P deposited graphite was studied in various concentrations of dextrose in 0.1 M KOH solution. Electroless Ni–P graphite showed higher catalytic effect for oxidation of dextrose when compared to pure Ni powders. The difference in performance can be attributed to the graphite particles on which the NiP was coated, which helped to enhance the surface area of the composite. The ECE for Ni–P was found to be approximately three times higher compared to pure Ni powder for the highest dextrose concentration used in this study.

Acknowledgement The authors would like to express their gratitude to Prof. P. M. Prasad, Emeritus Scientist, NFTDC, for his valuable suggestions and guidance.

References

1. Barker D (1993) Trans Inst Metal Finish 71:121
2. Gawne DT, Ma U (1987) Mater Sci Technol 3:228
3. Gemmler A, Zbloch T, Gut H, Keller W (1990) Mechanism of electroless nickel deposition and its utilization in expert systems. In: Proc 77th AESF Annual Tech Conf, Boston, MA, 9–12 July, pp 595–608
4. Hickling A, Johnson D (1967) Electroanal Chem 13:100
5. Brenner A, Riddell GE (1946) Proceedings of the American Electroplater's Association
6. Zeng Y, Zhou S (1999) Electrochem Commun 1:217
7. Yu P, Ritter JA, White RE, Popov BN (2000) J Electrochem Soc 147:1280
8. Yu P, Ritter JA, White RE, Popov BN (2000) J Electrochem Soc 147:2081
9. Montilla F, Morallón E, Vázquez JL, Alcañiz-Monge L, Cazorla-Amorós D, Linares-Solano A (2002) Carbon 40:2193
10. Paseka I (1995) Electrochim Acta 40:1633
11. Paseka I (1999) Electrochim Acta 44:4551
12. Podesta JJ, Piatti RCV, Arvia AJ (1992) Int J Hydrogen Energy 14:9
13. Fundo AM, Abrantes LM (2007) J Electroanal Chem 600:63
14. Kretz F, Gasci Z, Kovacs J, Pieczonka T (2004) Surf Coat Technol 180:575
15. Lin YJ, Jiang BF (1998) J Am Ceram Soc 81(9):2481
16. Kong FZ, Zhang XB, Xiong WQ et al (2002) Surf Coat Technol 155:33
17. Zhan-Min Q (2005) Electroplat Finish 24(2):21
18. Palaniappa M, Veera Babu G, Balasubramanian K (2007) Mater Sci Eng A (in press). DOI 10.1016/j.msea.2007.03.004
19. Scholz F, Schröder U, Gulaboski R (2005) In: Electrochemistry of immobilized particles and droplets. Springer, Heidelberg, Germany
20. Xinguo H, Naichao L (1990) In: A study of the kinetics of electroless composite plating. Proceedings of Asia Pacific Inter Finish '90, The Australian Institute of Metal Finishing, Melbourne, pp 26.1–26.9
21. Palaniappa M, Seshadri SK (2007) J Mater Sci (in press). DOI 10.1007/s10853-007-1501-5
22. Jayalakshmi M, Radhika P, Phani Raja M, Mohan Rao M (2007) J Solid State Electrochem 11:165
23. Jayalakshmi M, Venugopal N, Ramachandra Reddy B, Mohan Rao M (2005) J Power Sources 150:272
24. Shervedani RK, Lasia A (1997) J Electrochem Soc 144:511
25. Narayanan SS, Scholz F (1999) Electroanalysis 11:465
26. Scavetta E, Berreffoni N, Giorgetti M, Tonelli D (2002) Electrochim Acta 47:245
27. Yi Q, Zhang J, Huang W, Liu X (2007) Cat Commun 8:1022
28. Berchmans S, Gomathi H, Rao GP (1995) J Electroanal Chem 394:267
29. Fleischmann M, Korinek K, Pletcher D (1971) J Electroanal Chem 364:209
30. Fleischmann M, Korinek K, Pletcher D (1982) J Chem Soc Perkin Trans 2:1396